N90-28621

POOL BOILING FROM ROTATING AND STATIONARY SPHERES IN LIQUID NITROGEN

Winston M. Cuan and Sidney H. Schwartz

Rockwell International/Rocketdyne Division
Canoga Park, California

ABSTRACT

Results are presented for a preliminary experiment involving saturated pool boiling at 1 atmosphere from rotating spheres, 2 and 3 in. in diameter, which were immersed in liquid nitrogen (LN_2). Additional results are presented for a stationary, 2-in.-diameter sphere, quenched in LN_2, which have been obtained utilizing a more versatile and complete experimental apparatus that will eventually be used for additional rotating sphere experiments. The speed for the rotational tests was varied from 0 to 10,000 rpm. The stationary experiments parametrically varied pressure and subcooling levels from 0 to 600 psig and from 0 to 50°F, respectively. During the rotational tests, a high speed photographic analysis was undertaken to measure the thickness of the vapor film surrounding the sphere. The average Nusselt number over the cooling period was plotted against the rotational Reynolds number. Stationary sphere results included local boiling heat transfer coefficients at different latitudinal locations, for various pressure and subcooling levels.

INTRODUCTION

The main shaft ball bearings in the Space Shuttle Main Engine (SSME) high pressure oxidizer turbopumps (HPOTP) are exposed to high temperatures because of frictional heating during operation, resulting in bearing ball discoloration. To improve the heat removal mechanism from these balls, it is necessary to better understand the boiling heat transfer phenomenon associated with rotating balls in a cryogenic fluid. Furthermore, an exhaustive literature search was conducted to identify heat transfer correlations related to pool and forced-convection boiling from quenched spheres. Several correlations were found, but none encompass all of the independent parameters required for this application such as rotational speed and pressure. As a result, an extensive experimental investigation was initiated to better understand the effect of rotation, coolant pressure, and subcooling level on boiling heat transfer from spherical surfaces.

The primary objective of this experimental program was to parametrically study the effect of ball rotational speed, coolant pressure, and subcooling on boiling heat transfer from a heated sphere quenched in a

*Work reported herein was sponsored by NASA/Marshall Space Flight Center under Contract NAS8-40000.

liquid nitrogen (LN_2) bath. The experimental program used spheres of two different sizes to obtain ball surface velocities and centrifugal forces in the same range as those experienced in the HPOTP ball bearing. In addition, the ball was made of 440C CRES material, which is identical to the engine's bearing balls. Because of safety reasons, liquid nitrogen was used as the test liquid, as the thermodynamic and transport properties are similar to those of liquid oxygen (engine coolant). The range of pressures studied was varied from atmospheric to supercritical. The effect of cross flow was not included in this first phase of the study, although it is recognized that it eventually must be incorporated into the experiments in order to closely simulate the SSME bearing environment. The rotational speed was varied from 0 to 10,000 rpm, at which speed the 3-in. ball rotated at 67 percent of the equivalent surface speed for the 0.5-in. engine ball.

TEST APPARATUS

The early quench tests were carried out with a rotating sphere under atmospheric conditions. Since thermocouples were not attached, only the total elapsed quench times until the ball cooled to the point of transition boiling were recorded. The second phase of testing under pressure required a much more involved test facility. This facility is capable of testing over a range of pressures, rotational speeds and levels of liquid subcooling. Both of these facilities were designed and built for quench tests in a pool of LN_2.

First Phase

The first phase study basically provided overall cooling times for a rotating sphere quenched in LN_2. The test apparatus (Fig. 1) for this phase consisted of a dewar, motor, and ball. The glass dewar was a 10-in.diameter, 9-gal, double-wall, vacuum-sealed flask. Quenching was accomplished after heating the sphere in air and then raising the LN_2 glass dewar to immerse the sphere. A hydraulic unit was used for this purpose. 440C stainless steel spheres (2- and 3-in. diameter) were used in these tests. A 3/8-in. OD., hollow, Inconel 625 shaft connected the motor to the ball. A 1/2 hp variable speed motor, capable of achieving speeds up to 10,000 rpm, was used to rotate the shaft and the sphere.

High speed motion picture cameras were also employed in this phase of testing to observe the physical phenomenon along with the quantitative measurements. The photographic analysis was accomplished using both Fastax and Hycam high speed motion picture cameras to record the boiling phenomenon. Frame rates from 400 to 10,000 frames/sec were used in these experiments. Various combinations of front and silhouette back lighting were tried along with various fields of view to optimize the photographic results.

Second Phase

The second phase test facility was considerably more complex than that of the first phase. The liquid container had to maintain super-

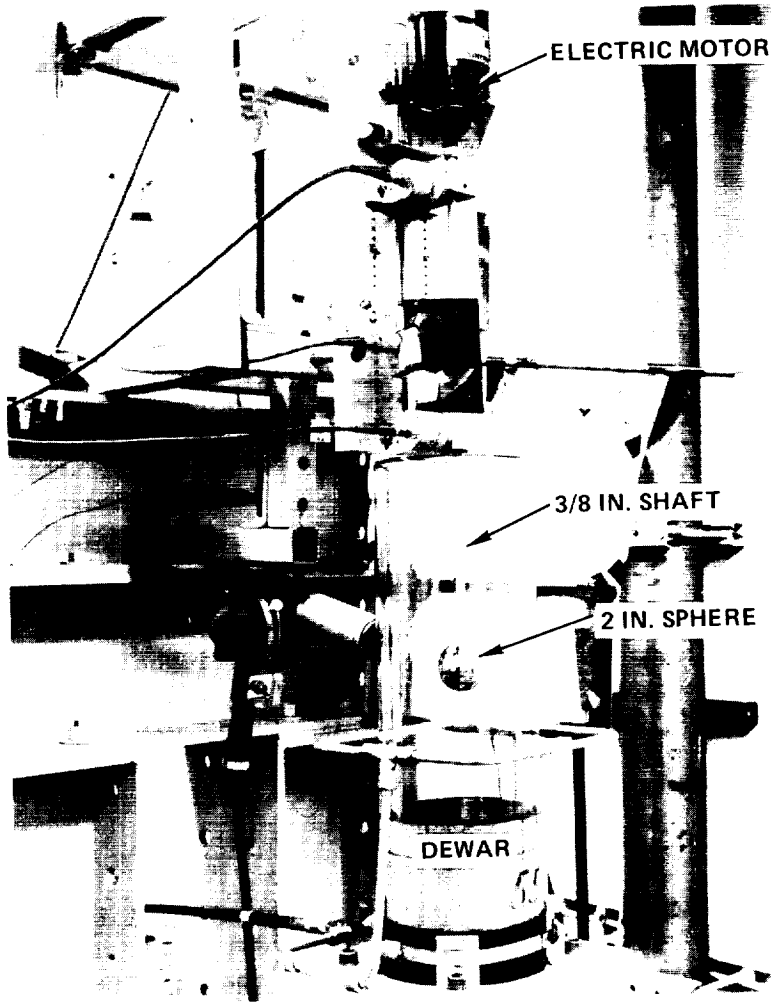

Fig. 1. Rotating Sphere Test Facility

critical pressures in addition to allowing for rapid pressurization after the sphere was heated. Furthermore, the pressure vessel had to be raised and lowered as in the first phase, while the pressure in the container was maintained relatively constant. Also, a pressurized, low-flow, liquid-feed system connected to the inner container was needed to maintain a constant pool temperature during sphere cooldown. Finally, windows in the container were required for both test monitoring and photographic analysis. Figure 2 shows an overall view of the apparatus employed in this study.

A pressurized, cylindrical steel container (10-in. diameter) was specifically made for this test program. An open-glass beaker, 7 in. in diameter and having a capacity of 6.5 gal, was placed inside this pressure vessel to hold the liquid. The pressurized feed system was used both for filling and for maintaining a constant bath temperature. The slow-moving coolant was continuously introduced into the bottom of the glass container, and was allowed to overflow into an annulus formed

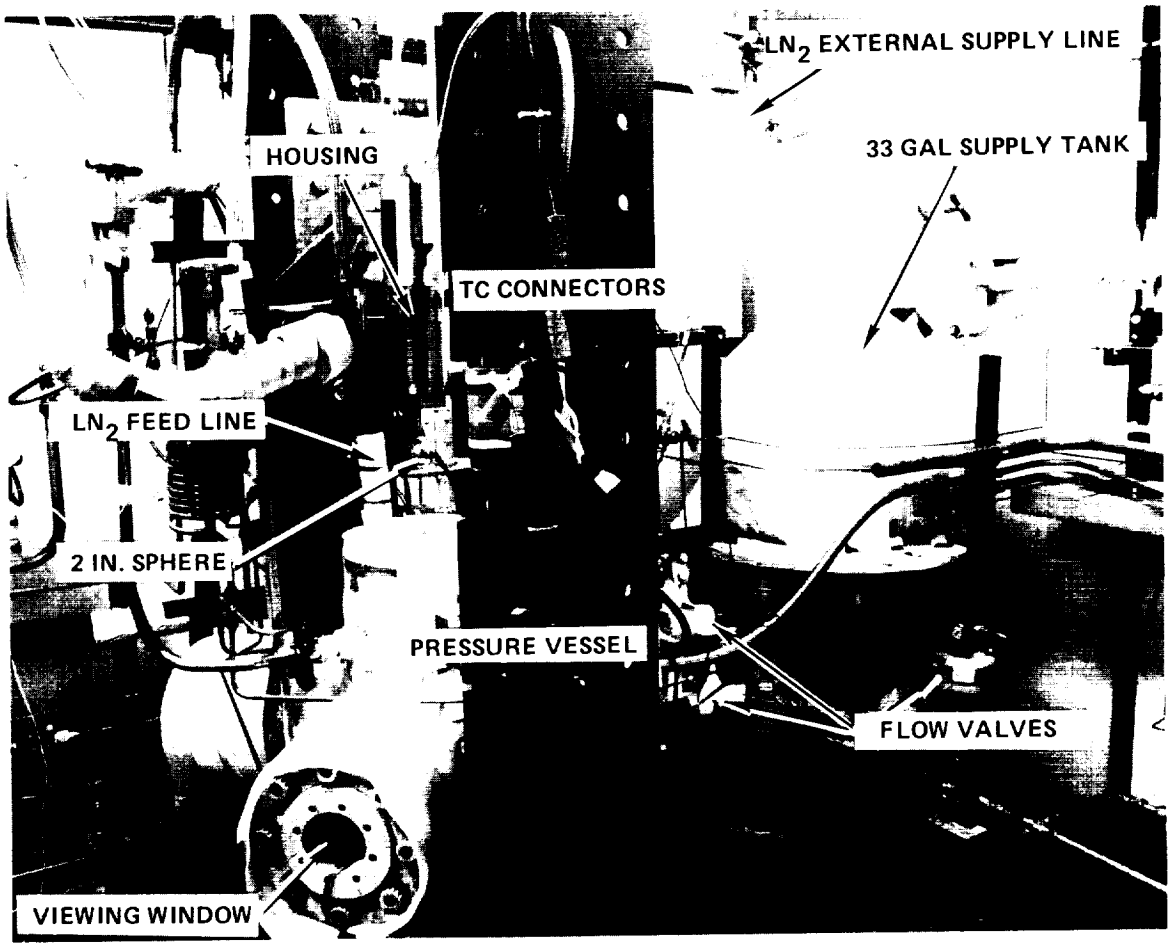

Fig. 2. Overall View of Stationary Sphere Test Facility

between it and the pressure vessel inside wall. The surplus LN_2 was then evacuated from the vessel base to a receiving tank. The feed system was capable of operating at all pressures and liquid temperatures. Liquid nitrogen was furnished to the test supply tank, with a capacity of 33 gal, from an external storage tank. The test supply tank and feed lines were insulated. The LN_2 temperature in the supply tank was controlled both by pressure and the amount of warm gaseous nitrogen (GN_2) injected into the bottom of the tank. The temperature of the LN_2 slowly rose after pressurization, advancing toward the equivalent saturation temperature. Figure 3 shows the schematic of the flow system. A highly polished, 2-in. diameter sphere made of 440C stainless steel material was used for the boiling experiments. Sheathed and grounded thermocouples were used to measure the ball temperature-time history during cooldown as well as to estimate the heat transfer from the surface of the ball. The thermocouples were radially positioned in pairs at various latitudinal locations on the sphere. One thermocouple from each pair was located flush with the surface and the other was located radially inward between 0.20 to 0.5 in. depending on the location. The sphere was X-rayed to accurately

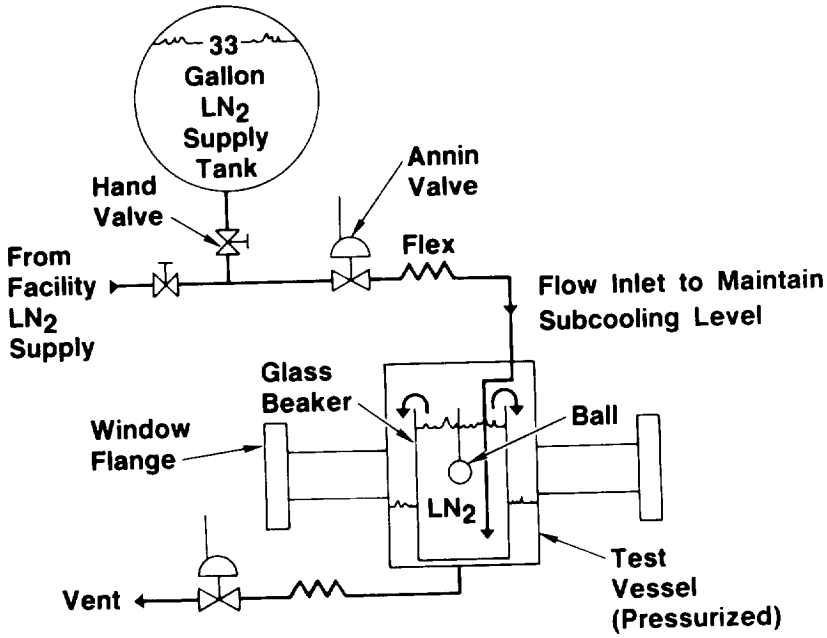

Fig. 3. Schematic of Stationary Sphere Test Rig With LN_2 Feed System

determine the thermocouple positions. Nine thermocouples, 0.02-in.in diameter, were brazed into holes made in the sphere. The thermocouple lead wires were routed through the hollow, 3/8-in. diameter, Inconel 625 shaft to the data acquisition system. When the rotational test phase begins, the thermocouple will be attached to slip ring connectors, which in turn will be connected to the data acquisition system. Figure 4 shows the sphere instrumentation locations.

In addition, three thermocouples were placed in the liquid bath at elevations above, below, and at the sphere's equator to check the LN_2 bulk temperature in the vicinity of the sphere. Two thermocouples were also installed inside the supply tank to control the subcooling level of the nitrogen before each test. Pressure transducers were placed inside the pressure vessel and in the supply tank.

The data acquisition system consisted of two major components: (1) the reference junction box and (2) the Hewlett Packard system 4000 acquisition system. The thermocouples leads from the sphere were connected to the reference junction box to provide a common junction for accurate temperature readings. The reference temperature was 150 $\pm 1^{o}F$. The output of the box, in millivolts, was in turn sent to the system 4000. The scanning rate of the system 4000 was 30 channels/sec. The system 4000 recorded the 18 test parameters (temperature and pressure measurements) at every 1.97-sec interval. Internally, the input signal passed through three stages. First, the signal was amplified by a factor of 10 using an amplifier. The precalibration amplifier's accuracy is ± 6.1 microvolts, which corresponds to approximately $\pm 0.3^{o}F$

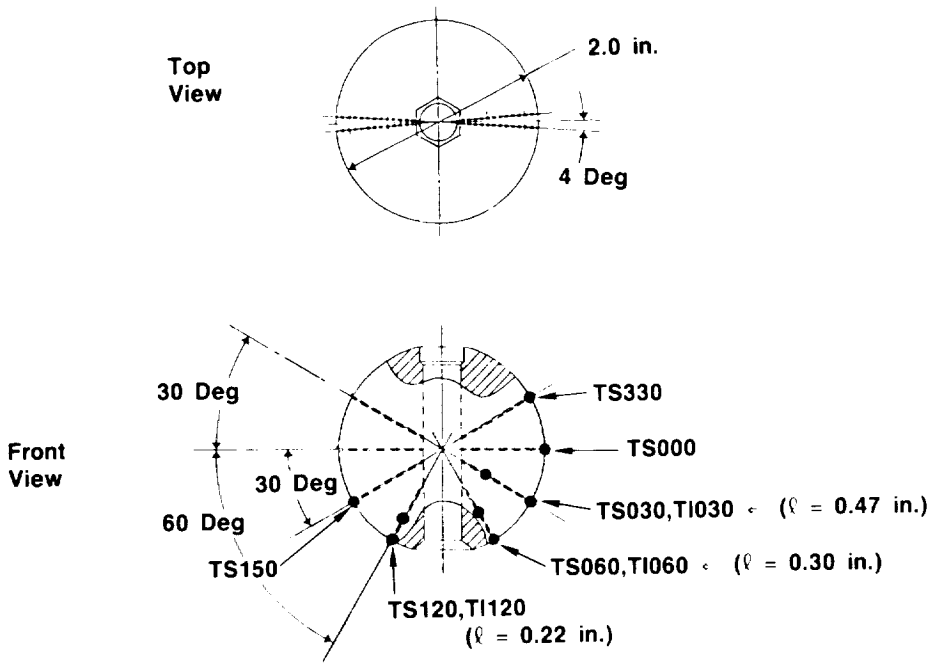

Fig. 4. Sphere Instrumentation Locations for Stationary Testing

during most of test duration, and to $\pm 0.6^{o}F$ in the nonlinear domain which occurred briefly near the end of the test. After the amplification, the signal was digitized using a 14 bit analog to digital converter. Finally, the digitized data was transferred into a personal computer's floppy disk and eventually transformed into an IBM format ASCII file for posttest processing.

To minimize the overall uncertainly of the data acquisition system, a customized calibration was performed with a temperature range varying from -320 to $212^{o}F$. A Doric unit with type-T thermocouples was the standard utilized for the calibration. In addition to four fixed temperature settings: saturated liquid nitrogen ($-320^{o}F$), a mixture of dry ice and alcohol ($-100^{o}F$), ice water ($-32^{o}F$), and boiling water ($212^{o}F$), intermediate steps between $-320^{o}F$ and $-232^{o}F$ were traversed. The technique consisted of pressurizing the liquid nitrogen from saturation to its critical pressure in increments of 50 psia, letting it reach the equivalent saturation temperature at each step. Calibration data revealed that thermocouples temperature readings agree closely with the above-mentioned standard used and hence only minor adjustments were required. Following these adjustments, the accuracy of the thermocouple improved to approximately $\pm 0.15^{o}F$.

TEST PROCEDURE

Rotating Tests

The glass dewar was filled with LN_2 such that the liquid level was at least 4 in. above the sphere. The initial temperature of the sphere was held close to 70°F prior to the start. Once the electric motor reached the selected speed, the glass dewar was raised by the hydraulic unit to immerse the sphere in liquid nitrogen. A chronometer was used to measure the time until the transition boiling regime was reached. This termination time was rather easy to recognize, as once the continuous vapor film was disrupted, frictional drag on the ball increased dramatically, causing violent swirling of the liquid in the dewar (Fig. 5). Prior to this time (during film boiling), the bulk liquid was hardly affected by the rotating sphere. Upon termination of a test the dewar was lowered, the motor turned off and the sphere warmed up to ambient temperature in preparation for the next test. Prior to each test the ball was hand polished as needed and carefully cleaned with either freon, alcohol, or acetone.

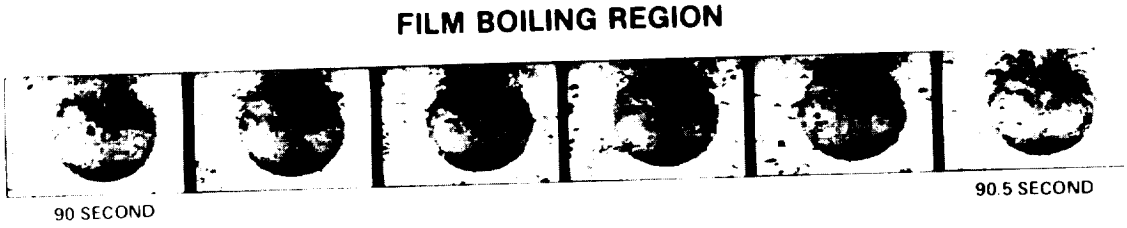

Fig. 5. Flow Visualization Results From 2-in Rotating Sphere (Rotational Speed = 6500 rpm)

Stationary and Pressure Tests

The pretest preparation was rather complex for this series of experiments. After filling and topping off the supply tank, the test pressure vessel and the feed lines were chilled down. The data acquisition system was pre-zeroed and the hydraulic lifting unit turned on. The pressure vessel was then raised by hydraulic cylinders until the static seal engaged around the housing cylindrical section. The pressure vessel and the supply tank were pressurized to a selected pressure level, maintaining a 10 to 20 psig differential between them. The feed system was activated by opening the flow valves, to allow liquid nitrogen to slowly

flow into the bottom of the inner glass container. Recording of the data was initiated prior to start of the flow and maintained until the end of the test, at which time the sphere surface temperatures reached the liquid temperature. The liquid nitrogen subcooling level and pressure were independently and steadily controlled throughout the test. A VHS video system allowed remote viewing of the sphere through one of the three glass viewing windows. A videotape was produced to record each experiment in its entire duration.

RESULTS AND DISCUSSION

Rotating Tests

Over 80 trials involving 2- and 3-in. spheres were conducted, varying the rotational speed from the stationary condition up to 10,000 rpm, in 1000 rpm increments. Thirty-seven of those trials were used for data reported herein. The remainder were used for repeatability, verification, photographic coverage, and apparatus checkout.

A photographic analysis was undertaken with both Fastax and Hycam high speed motion picture cameras with a variety of rotational speeds, camera frame rates, and different fields of view. An analysis of the film was used to determine the average thickness of the wavy vapor film, encompassing the 2-in. sphere. This analysis showed that the thickness is between 0.030 and 0.050 of an inch, for the 6000 rpm rotational speed. Furthermore, it was observed that the stable film boiling collapse always occurred at the top of the sphere first, and quickly progressed downward over the sphere.

The average heat transfer rates were computed by considering the sphere as a lumped-parameter system since the sphere experienced a relatively mild thermal transient during film boiling, which constituted the bulk of the test time.

The lumped-mass equation was used to find the average film heat transfer coefficient (h) as a function of the beginning and final sphere temperatures, and the cooling time. The end temperature was assumed to correspond to the minimun heat flux, as once the continuous vapor film is disrupted, the fluid friction between the rotating sphere and the LN_2 increases significantly causing the liquid in the dewar to rotate rapidly. The sphere's temperature at this minimum heat flux can only be assumed to be the same as that for a stationary sphere, which was recorded to be approximately $70^{o}F$ above the saturation temperature. Furthermore, Weaver (Ref. 1), did show that there was no significant shift in this temperature, corresponding to the minimum heat flux, with rotational speed for a sphere inmersed in freon 113.

Calculated values of h were made dimensionless and the resulting average Nusselt number values were plotted against the rotational Reynolds number, which was based on the sphere's tangential velocity

and nitrogen's vapor kinematic viscosity. The following equations were used to calculate $\bar{h}$, $\bar{Nu}$ and Re

$$\bar{h} = - \frac{\rho V C_p}{A \Delta t} \ell n \frac{T_f - T_s}{T_o - T_s}$$

(where ρ and C_p are based on 440C CRES material properties.)

$$\bar{Nu}_v = \frac{\bar{h} D}{k_v}$$

and

$$Re_v = \frac{R \omega D}{\nu_v}$$

The data are shown in Fig. 6 . As noted, the Nusselt number appears to be insensitive to the Reynolds number up to a value of approximately 10^6. Then, the Nusselt number begins to rise as the Reynolds number increases. This is felt to occur when the rotational velocity or inertia effect begins to be important with respect to the buoyancy force as a heat removal mechanism.

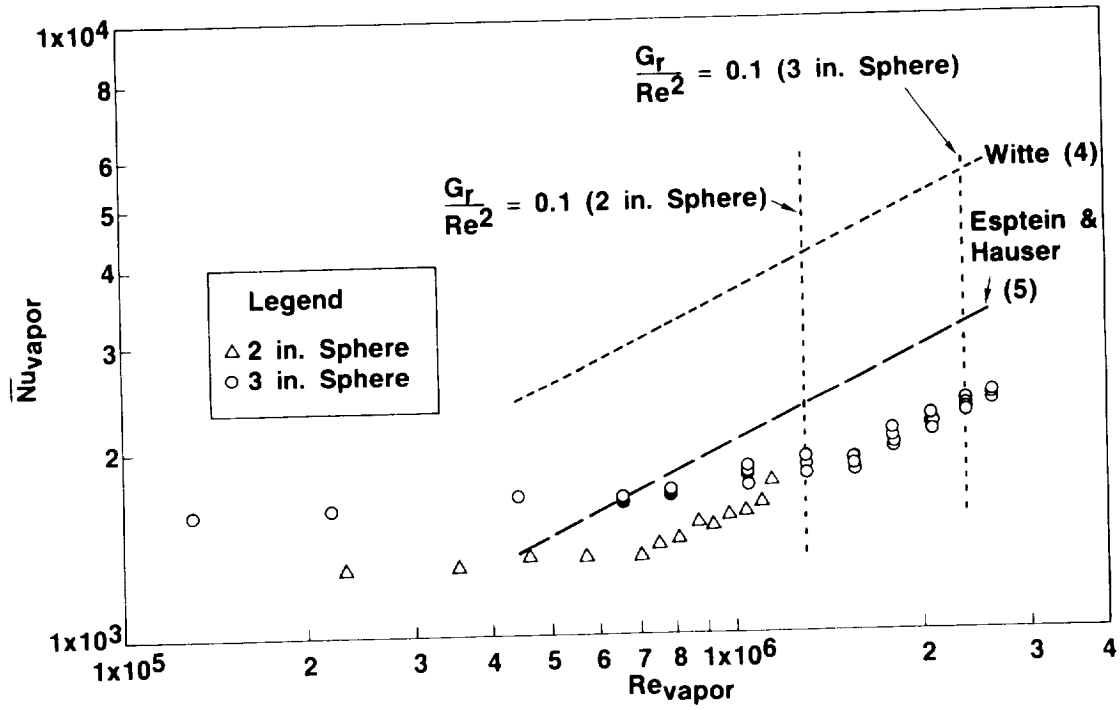

Fig. 6. Experimental Results of Rotating Noninstrumented 2- and 3-in. Spheres

The determination of the value of this critical Reynolds number as well as the trend of the data in the rotationally dominated regime is considered below.

Kreith (Ref. 2) has confirmed that for $(Gr/Re^2) < 1/10$, the natural convection effects can be ignored for single-phase heat transfer from a rotating sphere. This same criterion is used here for the pool film boiling (two-phase flow), where both the inertia and bouyancy effects are based on vapor properties. The use of vapor properties is based on observations of the liquid nitrogen bath, appearing nearly motionless, when a rotating sphere surrounded by a vapor film, is rotating within it. The following expression defines the dimensionless ratio $(Gr/Re^2)_v$:

$$\left(\frac{Gr}{Re^2}\right)_v = \frac{\dfrac{g\,(\rho_\ell - \rho_v)\,D^3}{\rho_v\,\nu_v^2}}{\left(\dfrac{U_t\,D}{\nu_v}\right)^2} \tag{1}$$

which can be rewritten as:

$$\left(\frac{Gr}{Re^2}\right)_v = \frac{\dfrac{\rho_\ell}{\rho_v}}{\dfrac{U_t^{\,2}}{gD}} \tag{2}$$

where the following approximation was made above: $(\rho_\ell - \rho_v) \simeq \rho_\ell$.

Figure 6 shows the values of Re_v based upon Eq. (2) and the dimensionless ratio $(Gr/Re^2)_v < 1/10$. When this inequality is satisfied, the bouyancy effects are unimportant for both the 2- and 3-in. diameter spheres. As can be seen, the predicted values of Re_v, where this transition occurs, agree quite well with the data.

It should be noted that earlier work with flow film boiling over a stationary cylinder, as discussed by Hasan et al. (Ref. 3), the criterion $U_\infty/(gD)^{1/2} > 10$ was used instead. This criterion results from the assumption that the dimensionless ratio (Gr/Re^2) is based on the liquid properties for ρ and ν. As seen from Eq. (2), this would imply that the equivalent (Gr/Re^2), based on vapor properties, be equal to $(\rho_\ell/\rho_v)/100$, which for the case of LN_2 at atmospheric condition leads to $(Gr/Re^2)_v = 1.5$. This value is much greater than 0.1 used in Fig. 6, indicating that the critical Reynolds number, at which point the rotationally dominated regime begins, is underestimated by an order of magnitude using Hasan et al.'s criterion.

Comparison With Existing Correlations

The only possible comparison of the present data with existing correlations can be made by replacing the free stream velocity (U_∞) with the tangential velocity (U_t) in a forced flow boiling correlation. Two separate equations for saturated flow film boiling over a stationary sphere are included below.

Witte (Ref. 4) developed one of those equations from theory and modified the constant with test data. The resulting equation is

$$Nu = \frac{2.98\ Re_v^{1/2}}{\left(\frac{C_{p,v}\ \Delta T_w}{Pr_v\ h'_{fg}}\right)^{1/2}} \tag{3}$$

Witte's theoretical equation had the constant 0.698 instead of 2.98.

Another equation obtained from analysis by Epstein and Hauser (Ref. 5) is based upon the stagnation region, but is used here for comparison. Their equation is

$$Nu = \frac{0.553\ Re_v^{1/2}\left(\frac{\rho_\ell}{\rho_v}\right)^{1/4}}{\left(\frac{C_{p,v}\ \Delta T_w}{Pr_v\ h_{fg}}\right)^{1/4}} \tag{4}$$

Both equations are plotted on Fig. 6, where the Reynolds number is based on U_t, rather than U_∞. Surprisingly, the two equations bracket the rotating sphere data, which lends some credibility to the substitution of U_t for U_∞ in the the Reynolds number, as a method of finding the film coefficient for a rotating sphere using a conventional forced convection correlation. However, it should be noted that, there is no solid basis for replacing the free stream velocity in a flow boiling correlation with the tangential velocity for a rotating sphere in a stagnant pool. Furthermore, it should be reiterated that, for the film coefficient values reported here, it was assumed that h remained constant over the entire cooling period in the film boiling regime. These assumptions may contribute to deviations observed between the correlations and the test data, although fairly good agreement was noticed. It should be noted that Irving and Westwater (Ref. 6) showed that boiling results were quench-rate independent for spheres 2 in. in diameter or larger.

STATIONARY AND PRESSURE TESTS

In excess of 70 trials were conducted using an instrumented, 2-in sphere and varying the liquid nitrogen pressure, subcooling level, and sphere's initial temperature. The pressure was varied from 0 to 600 psig (supercritical), the subcooling from 0°F (saturation) to 50°F, and the sphere's initial temperature from 70°F (room temperature) to 450°F. Table 1 shows the test matrix with selected tests accomplished for this phase.

Table 1. Text Matrix for Stationary Sphere

Subcooling Temperature (F)	Pressure (psig)							
	0	50	100	200	300	400	500*	600*
0	1-5 1-63 1-67	1-62	1-18 1-47	1-11 1-49	1-46 1-56	1-44 1-50 1-75		
10		1-61	1-25 1-43 1-53	1-19 1-30 1-34	1-26 1-41 1-58	1-17 1-33 1-51	1-64	1-35 1-60
20				1-4 1-29 1-42	1-24 1-31	1-12 1-40 1-59		1-15
30				1-32	1-23 1-36	1-21 1-27 1-57	1-65	1-14 1-16
40					1-10 1-22 1-55	1-13 1-37 1-39 1-45 1-48 1-52		1-28
50						1-6 1-38	1-7	1-66

*Subcooling level based on the saturation temperature at critical pressure

Local film coefficients were determined based upon the radial temperature gradient, measured from several pairs of thermocouples located at various latitudinal locations. The data reduction was based on an energy balance applied to an element encompassing each thermocouple pair. The expression for the heat flux per unit area is given as:

$$q/A = \frac{k}{\ell}\left(T_{TC,I} - T_{TC,S}\right) - \rho \frac{C_p \ell}{2} \frac{\Delta T_{TC,S}}{\Delta t} \qquad (5)$$

where the thermodynamic properties for the sphere are based on 440C CRES material for k, C_p and ρ.

Figure 7 displays typical test data in terms of film coefficient (h) versus sphere surface temperature for the location 30-deg below the equator, for various pressure levels. It can be seen that film coefficient increases as the LN_2 pressure is increased from saturation to supercritical levels. The major changes in h occur when the pressure increases from 0 to 200 psig, and subsequently the rate of change is less as the critical pressure is reached. Also, there is a sharp increase in h as the pressure becomes supercritical.

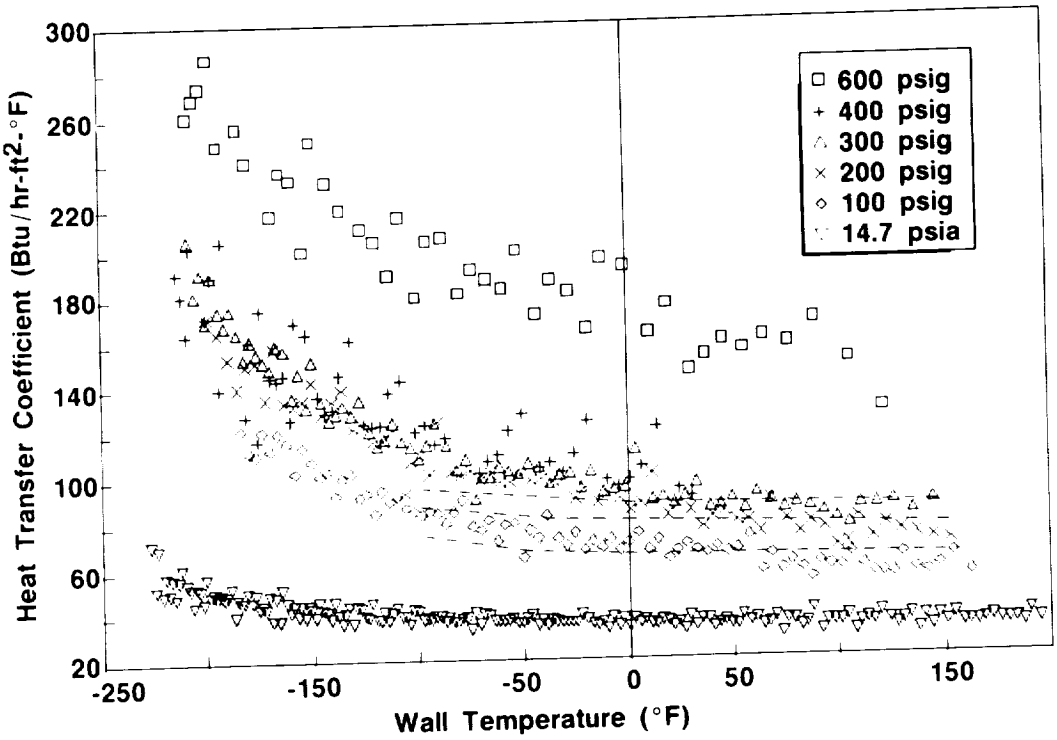

Fig. 7. Film Coefficient vs Surface Temperature for Various Pressure Levels at 10°F Subcooling For a Location 30-deg Below the Equator

Figure 8 shows test data expressed in the form of h as function of wall temperature for various LN_2 subcooling levels. The film coefficient is modestly affected by changes in subcooling level; although there appears to be a negligible change above the 30 degrees subcooled condition.

Comparison of Stationary Sphere Data With Pool Film Boiling Correlations

Few correlations associated with subcooled pool film boiling have been found in the literature. Two of those found, based upon boiling from a stationary cylinder, are compared with the present data for a sphere. Witte (Ref. 4) discussed similarities in film boiling for both geometries.

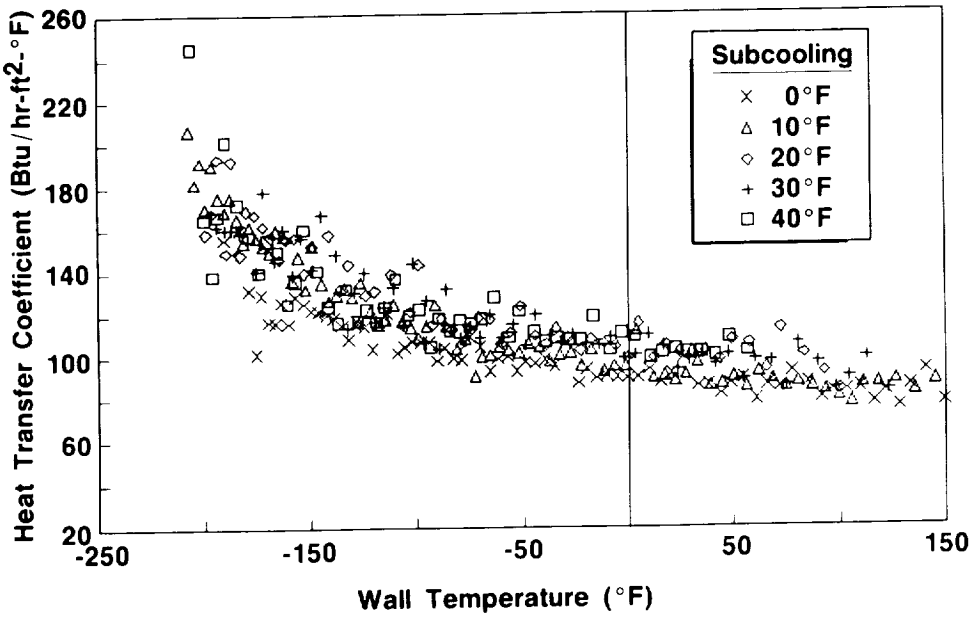

Fig. 8. Film Coefficient vs Surface Temperature at Constant Pressure for Various Subcooling Levels at 30 Degrees Below the Equator (300 psig)

The correlation given by Sakurai, et al (Ref. 7) was examined and found to show a decrease in the film coefficient with an increase in the subcooling level. This contradicts other data found in the literature as well as data presented herein. Consequently, no other consideration was given to this correlation.

On the other hand, Siviour and Ede's correlation (Ref. 8) was found to predict trends shown by other data as well as that of this study. Their equation, neglecting radiation losses is:

$$q_w = 0.613 \frac{k_v}{D} \Delta T_w \left(Gr_v \, Pr_v\right)^{1/4} \left(\frac{l}{Sp}\right)^{1/4} + 0.59 \frac{k_\ell}{D} \Delta T_{SC} \left(Gr_\ell \, Pr_\ell^2\right)^{1/4} \quad (6)$$

where the terms in the above equation are defined in the Nomenclature section.

Results obtained with Eq. (6) are shown as dashed lines in Fig. 7 for pressure levels of 100, 200, and 300 psig and with a subcooling level of 10°F. However, both constants in Eq. (6) were adjusted upward to fit the test data. The correction factor used is equal to 1.6. Considering the difference in geometry between a cylinder and a sphere, such an adjustment would not be surprising and, in fact, Witte (Ref. 4) utilized it. As noted in Fig. 7, the effect of pressure on h

from results obtained with the modified Eq. (6) is in reasonably good agreement with the trend displayed by the test data. However, the test data begin to deviate significantly from the correlation when the wall temperature is below $-100^{o}F$.

CONCLUSIONS

The rotating sphere saturated pool film boiling test results tend to agree with results obtained from forced flow boiling correlations when tangential velocity replaces crossflow velocity.

The subcooled pool film boiling test data for a sphere show a substantial increase in the film coefficient with pressure rise through supercritical pressures.

The subcooled pool film boiling test data for a sphere exhibit a modest increase in the film coefficient as the subcooling level increases.

NOMENCLATURE

A	=	area of sphere
C_p	=	specific heat
D	=	diameter of sphere
g	=	gravitational constant
Gr	=	Grashof number
h	=	film coefficient
h_{fg}	=	latent heat of vaporization
h'_{fg}	=	$h'_{fg} = h_{fg} + 0.5\ C_{p,v}\ \Delta T_w$
k	=	thermal conductivity
ℓ	=	thermocouple spacing
LN_2	=	liquid nitrogen
Nu	=	Nusselt number
Pr	=	Prandtl number
R	=	radius
Re	=	Reynolds number
Sp	=	$Sp = C_{p,v}\ \Delta T_{SC}/h_{fg}$
T_b	=	bulk temperature
T_f	=	final sphere temperature
T_o	=	initial sphere temperature
T_s	=	saturation temperature
$T_{TC,I}$	=	thermocouple temperature inside the sphere
$T_{TC,S}$	=	thermocouple temperature at the surface
T_w	=	wall temperature
Δt	=	elapsed time
ΔT_{SC}	=	$T_s - T_b$
$\Delta T_{TC,S}$	=	surface thermocouple temperature drop over time period Δt
ΔT_w	=	$T_w - T_s$
U	=	velocity
V	=	volume of sphere

Subscripts

ℓ = liquid
t = tangential
v = vapor

Greek Symbols

ν = kinetic viscosity
ω = rotational speed
ρ = density

REFERENCES

1. Weaver, D., Pool Boiling From a Rotating Sphere in Fr-113, M.S. Project Report, Mechanical Engineering Department, California State University at Northride, May 1988.

2. Kreith, F., "Convection Heat Transfer in a Rotating System," Advances in Heat Transfer, Vol. 5, pp. 141-145.

3. Hasan, M. E., M. M. Hasan, R. Eichhorn, and J. H. Lienhard, "Burnout During Crossflow Over Cylinders Beyond the Influence of Gravity," ASME Journal of Heat Transfer, Vol. 103, pp. 478-484.

4. Witte, L. C., "Film Boiling From a Sphere," I&EC Fundamentals, Vol. 7, pp. 517-518, August 1968.

5. Epstein, M. and G. Hauser, "Subcooled Forced-Convection Film Boiling in the Forward Stagnation Region of a Sphere or Cylinder," Int. Journal Heat Mass Transfer, Vol. 23, pp. 179-189.

6. Irving, M. E. and J. W. Westwater, "Limitations for Obtaining Boiling Curves by the Quenching Method with Spheres," Proceedings of the 8th International Heat Transfer Conference, Vol. 4, pp. 2061-2066, Hemisphere Publishing Corporation, Washington D.C.

7. Sakurai, A. M. Shiotsu, and K. Hata, "Effect of Subcooling on Film Boiling Heat Transfer From Horizontal Cylinder in a Pool of Water," Proceeding of the 1986 International Heat Transfer Meeting, pp. 2043-2048.

8. Siviour, J. and A. Ede, "Heat Transfer in Subcooled Pool Film Boiling," Heat Transfer - 1970, Vol. V, B3.12, Elsevier Publishing Company, Amsterdam, 1970.